Journal of Hydrology 623 (2023) 129843

Contents lists available at ScienceDirect

Journal of Hydrology

journal homepage: www.elsevier.com/locate/jhydrol

Research papers

Forest canopy interception can reduce flood discharge: Inferences from model assumption analysis

Hiroki Momiyama [a,b,*], Tomo'omi Kumagai [b,c,d], Naoya Fujime [b], Tomohiro Egusa [e], Takanori Shimizu [a]

[a] Forestry and Forest Products Research Institute, Forest Research and Management Organization, Tsukuba, Japan
[b] Graduate School of Agricultural and Life Sciences, The University of Tokyo, Tokyo, Japan
[c] Institute for Space-Earth Environmental Research, Nagoya University, Nagoya, Japan
[d] Water Resources Research Center, University of Hawai'i at Mānoa, Honolulu, USA
[e] Faculty of Agriculture, Shizuoka University, Shizuoka, Japan

ARTICLE INFO

Keywords:
Forest management
Low flow
Flood control
Interception
Rainfall partitioning
Water balance model

ABSTRACT

Some interception (IC) models assume proportionality between the IC and rainfall amount during heavy rainfall, while others do not. Although differences in the assumptions of the IC model can significantly impact water balance and runoff prediction, quantitative analysis has not yet been conducted. In this study, we investigated the influence of IC model selection on runoff prediction and its parameter estimation in a forested catchment in Japan. First, an IC model was presented as a function that can continuously represent the case where the IC increases with rainfall but asymptotically reaches a flat plateau and the case where IC is completely proportional to rainfall. The IC estimation using the model was compared with the IC data observed in 2020–2021 at three coniferous plantation plots within the catchment. Second, the IC model was incorporated into a catchment-scale water balance model (TOPMODEL-based tank model), and then the IC model that optimally reproduced the runoff observed in 2010–2015 was determined. The results showed that the observed IC and runoff were optimally reproduced when the IC was completely proportional to rainfall. However, it was observed that the assumption of the IC was not as influential on runoff predictability as the water retention capacity parameter of the catchment water balance model. Meanwhile, once the appropriate water retention capacity parameter was fixed, the impact of the difference in IC models on runoff prediction was significant at high-flow periods. Moreover, estimated high flow became large without the assumption that the IC was somehow proportional to rainfall, suggesting the importance of adequately representing the occurrence of IC, especially during heavy rainfall events. This implies that the IC by the forest canopy plays a significant role in controlling flood discharge from forested watersheds.

Abbreviations and Symbols: A, Contributing catchment area per unit contour length; a_i, Parameters determining runoff efficiency from a discharge hole i in the tank model framework; C, A height reference to make H and h_i positive; c_p, Heat capacity of air (J kg^{-1} K^{-1}); DBH, Diameter at breast height; $\overline{D}_s$, The catchment average saturation deficit; ET, Evapotranspiration; EF, Forest floor evaporation; f_s, A constant that defines the decrease in saturated hydraulic conductivity with depth; $f(P)$, The probability density function of daily P; G_s, Monthly mean surface conductance (mm s^{-1}); h_i, Parameters that determine the runoff efficiency from pore i in the tank model scheme; H, Current height of the water surface in the tank from the height reference in the tank model framework; IC, Interception; k_t, A time constant; m, A soil parameter used in the TOPMODEL framework that represents water retention capacity; n, Number of time steps; N, Number of discharge holes in the tank model scheme; NS, Nash–Sutcliffe efficiency criterion; NS_{inv}, Nash–Sutcliffe efficiency criterion with inverse Q values; OEW, Oborasawa Experimental Watershed; P, Rainfall amount; PAI, Plant area index; Q, Runoff; Q_m, Modeled Q; Q_o, Observed Q; RH, Relative humidity; $\overline{R}_s$, Monthly mean solar radiation (W/m^{-2}); R_s, Solar radiation; SD, Standard deviation; SF, Stem flow; S_T, Maximum value of the IC (or canopy storage capacity); t, Time (day); T_a, Annual mean air temperature; TF, Throughfall; TI, Topographic index; $\overline{TI}$, The catchment average TI; TI_i, TI at a given point i; T_{max}, A soil parameter representing transmissivity in the TOPMODEL framework; TR, Transpiration; VPD, Vapor pressure deficit; $\overline{VPD}$, Monthly mean vapor pressure deficit (kPa); β, Terminal interception ratio (interception ratio supposing $P \rightarrow \infty$); β_T, Total interception ratio (the ratio of total IC to total P throughout the concerning period); γ, Psychrometric constant (Pa K^{-1}); η_p, Mean P on wet days (mm day^{-1}); θ, Local slope; λ, The latent heat of vaporization of water (J kg^{-1}); ρ_a, The density of dry air (kg m^{-3}); ρ_w, The density of water (kg m^{-3}); ϕ, Soil porosity.

* Corresponding author at: Department of Disaster Prevention, Meteorology and Hydrology, Forestry and Forest Products Research Institute, Matsunosato 1, Tsukuba, Ibaraki 305-8687, Japan.
E-mail address: momiyamahiroki@affrc.go.jp (H. Momiyama).

https://doi.org/10.1016/j.jhydrol.2023.129843
Received 5 December 2022; Received in revised form 16 June 2023; Accepted 19 June 2023
Available online 21 June 2023

1. Introduction

The runoff (Q) from forested headwaters is imperative in supplying water resources and controlling flood discharge to the lower reaches, resulting from a balance between the catchment water storage and the water use by vegetation (Andréassian, 2004; Bosch and Hewlett, 1982). In particular, the forest water use by evapotranspiration (ET), which changes with the forest status, is a major determinant for Q from the headwater catchment (Komatsu and Kume, 2020). Thus, it has been expected that forest management and conservation activities can optimize Q, that is, maintain the low flow and control the high flow (Calder, 2007). Moreover, global warming is projected to increase the risk of climate extremes, including heavy precipitation and agricultural/ecological drought (IPCC, 2021). Under the present conditions, there is an increasing need for forest management and conservation to adapt to or mitigate climate change (Ellison et al., 2017; Sun et al., 2017).

Forest ET comprises canopy transpiration (TR), forest floor evaporation (EF), and interception (IC). Globally, TR, EF, and IC account for 64%, 6%, and 27% of total terrestrial ET, respectively (Good et al., 2015). Previous studies have suggested that in forests, TR combined with EF (comparable to plant transpiration combined with soil evaporation) is a conservative process because differences in forest stand status mainly affect TR and EF partitioning but not their sum (Delzon and Loustau, 2005; Komatsu, 2020; Oren et al., 1998; Roberts, 1983). Although the ratio of IC to ET was small compared to that of TR combined with EF, the IC was observed to have a linear relationship with the stem density of the plot (Komatsu et al., 2007). Moreover, many previous studies have suggested that IC is susceptible to changes in forest status resulting from forest management (Fan et al., 2014; Ghimire et al., 2012; Grunicke et al., 2020; Nanko et al., 2016; Shinohara et al., 2015; Sun et al., 2015; Takahashi et al., 2011). Hence, IC changes due to the alteration of forest status or forest management should be among the most important factors that control the rainfall-runoff process.

Here, we describe two mechanisms for rainwater loss to the atmosphere, that is, wet canopy evaporation by IC: the IC increases with the rainfall amount (P) and reaches a plateau (i.e., a certain amount of P would saturate the canopy storage) (Model 1), and the IC increases proportionally to P without a plateau (Model 2). The most commonly applied models are similar to Model 1 (Gash, 1979; Rutter et al., 1971), assuming that evaporation and drainage are from canopy storage. Although in such cases wet canopy evaporation is calculated using the Penman–Monteith equation (Muzylo et al., 2009), the calculated values have often been observed to be much smaller than the observations (see van Dijk et al., 2015). Notably, while some observations demonstrated that evaporation during rainfall events dominated the IC at the canopy (e.g., Murakami, 2021), Iida et al. (2017) observed that the intensity of IC in the first half of the rainfall events is higher than in the second half, implying the importance of the canopy water storage capacity for the IC estimation. The heat balance model's underestimation of the observed wet canopy evaporation is not very certain, including during rainfall events (see Carlyle-Moses and Gash, 2011; Guswa et al., 2020; Kumagai et al., 2014), which is the subject of this investigation.

As an endmember of the effect of the IC model selection, the presence or absence of a plateau in the IC estimation is critical for runoff prediction because it determines the input to the catchment water balance, especially during heavy rainfall events. Previous studies have assessed various potential ET models regarding runoff simulation efficiency, and they showed that simple potential ET models could work as well as precise ones (Bai et al., 2016; Oudin et al., 2005a, Oudin et al., 2005b). Furthermore, Fenicia et al. (2008) examined the effect of IC model application on a hydrological model, suggesting the importance of IC estimation in runoff prediction, including spatial distribution of storage for IC in the catchment. However, to the best of our knowledge, the extent of the impact due to different assumptions placed on the IC estimation on runoff prediction has not been investigated.

We aimed to assess how proper IC model selection affects the performance of the catchment water balance model. Thus, we used detailed catchment-hydrology observations conducted over six years, including IC data taken throughout the year at multiple plots and a semi-process-based catchment water balance model (a TOPMODEL-based tank model;

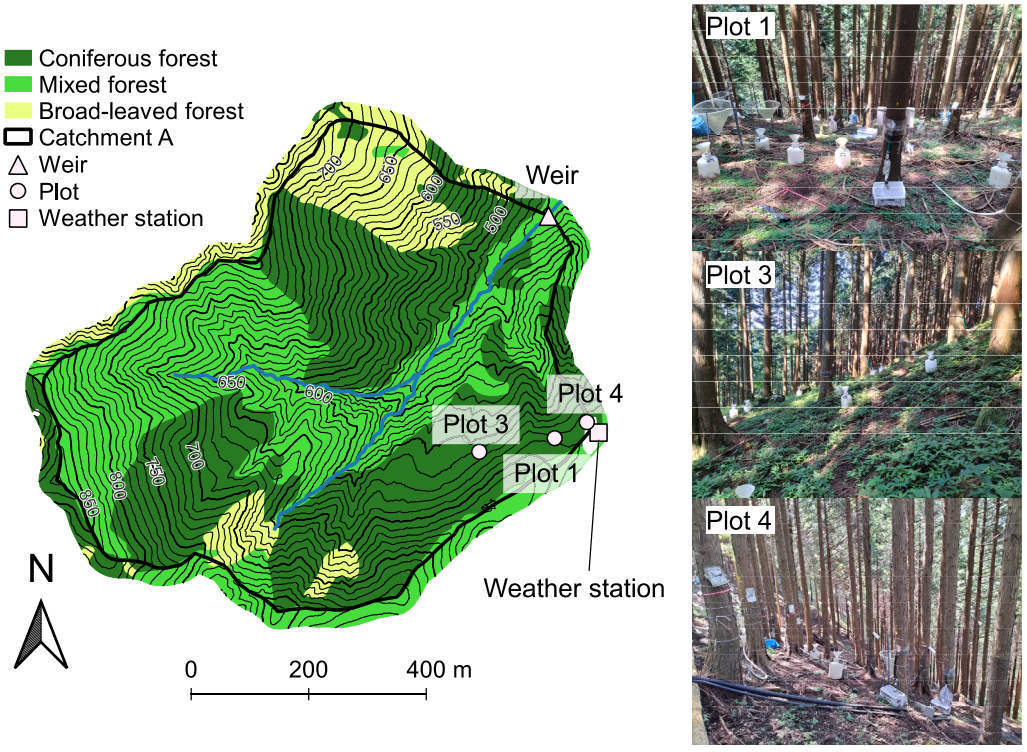

Fig. 1. Topography and vegetation of Catchment A, which is devoted to catchment-scale water budget observations in the Oborasawa Experimental Watershed. Locations and photographs of canopy interception measurement plots (Plots 1, 3, and 4) are also shown.

Table 1
Stand characteristics of Plots 1, 3, and 4 in Fig. 1.

Characteristics	Plot 1	Plot 3	Plot 4
Plot area (m^2)	297	130	203
Species	*Cr. japonica*	*Cr. japonica*	*Ch. obtusa*
Age (years)	35	65	35
Density (trees ha^{-1})	1280	780	1770
PAI [a] (m^2 m^{-2})	3.3–4.2	3.6–4.0	3.0–4.2
Mean DBH (cm)	27.3	42.2	24.0
Range DBH (cm)	17.2–33.7	34.1–66.0	15.5–32.5
Mean height (m)	20.9	26.0	17.5
Number of throughfall collectors [b]	14–18	11	7–11
Number of stemflow measurement trees	5	2	4

[a] Ranges of values denote seasonal variation.
[b] Ranges of values denote changes in the number of collectors during the observation periods.

cf. Beven and Kirkby, 1979; Momiyama et al., 2021). The IC at each rain event can be estimated with the observation as follows:

$$IC = P - TF - SF, \quad (1)$$

where TF and SF are the measured throughfall and stemflow over a plot during some rain events. The ratio of IC to P throughout a certain observation period (hereinafter, total interception ratio β_T) is a good indicator to describe the canopy property for the efficiency of the IC globally (Yue et al., 2021). Notably, we elaborated on the TF and SF observations and estimated the IC using Eq. (1). Here, three questions are raised: (1) Which IC model most accurately represents the observed IC—Model 1, Model 2, or a hybrid of them that is weighed according to their importance? (2) Which IC model best reproduces runoff characteristics estimated by the catchment water balance model? Is this the same as the model selected in (1)? (3) How does the accurate reproduction of actual IC by model selection improve modeled rainfall-runoff processes, especially the reproduction of high and low flows? The answers to these questions are important for incorporating IC into runoff prediction or for estimating the effect of IC on watershed management. This research will present new insights into the strategies for changing the IC through forest management to control high and low flows from forested headwaters.

2. Methods

2.1. Data

This study used the data obtained by IC observations from 2020 to 2021 and hydrological observations from 2010 to 2015. Canopy IC, meteorology, and rainfall-runoff data, which were well suited for the catchment water balance and ET model parameters, were obtained for a 49-ha forest headwater catchment (Catchment A) in the Oborasawa Experimental Watershed (OEW; 35°28′N, 139°12′E) in the Tanzawa mountains in the Kanto region of Japan (Fig. 1; Table 1). Forests in the OEW comprise mainly coniferous plantation stands, and the bare land ratio is less than 1%. Approximately two-thirds of the forested areas are composed of conifers (i.e., *Cryptomeria japonica* D. Don and, to a lesser degree, *Chamaecyparis obtusa* Endl). The remaining one-third is fragmented areas of deciduous broadleaved trees (e.g., *Cercidiphyllum japonicum* Sieb. et Zucc. and *Aesculus turbinate* Blume). The catchment is steep with a mean slope (±standard deviation [SD]) of 34.9 ± 9.0°. The soil was classified as Cambisol with a large portion of volcanic ash and a high infiltration capacity at the surface, and the mean soil depth (±SD) was 1.64 ± 0.97 m. The underlying bedrock beneath the soil is tuff, composed mainly of volcanic breccia, and is classified as Cenozoic rocks. There is a weathered bedrock with fissures below 40 m from the surface, and its hydraulic conductivity depends on the degree of weathering.

The annual mean air temperature (T_a) was 11.6 °C between 2010 and 2015, with an annual minimum daily mean T_a of − 3.0 °C around January and an annual maximum daily mean of T_a of 24.9 °C around August. The mean daily vapor pressure deficit (VPD) averaged over daylight hours (0600–1800 LT) reached a maximum of 1.7 kPa in May. Snowfall occurs only once or twice a year from January to March, accounting for only a small percentage of total annual P, and has limited influence on Q.

The data from the catchment-scale water budget observations from 2010 to 2015 were used to optimize the water balance model described later. Note that the Q data for the same period as the IC observations were not available due to Typhoon Hagibis, which hit Japan in October 2019. We confirmed that the annual bedrock drainage and intercatchment groundwater flow in the studied catchment could be negligible (see Egusa et al., 2021; Oda et al., 2013). Q from the studied catchment was measured using a V-notch weir. The weather station at the open ridge (Fig. 1) was devoted to above-canopy meteorological measurements, such as solar radiation (R_s), relative humidity (RH), T_a, and P. The VPD was calculated as a saturated vapor pressure of T_a minus an actual vapor pressure estimated from the RH. More detailed instrumentation information is provided elsewhere (Momiyama et al., 2021).

In the studied catchment, three plots were instrumented for SF (stem flow) and TF (throughfall) measurements (Fig. 1; Table 1). Plots 1 and 3 were established in stands of *Cr. japonica*, and Plot 4 was established in the *Ch. obtusa* stand; data obtained were used in the following analysis. P was measured with a 0.5 mm tipping-bucket rain gauge (CTKF-1, Climatec, Tokyo, Japan) on the top of the tower of the weather station and corrected by manual measurement with polyethylene plastic bottles at the weather station. In each plot, the TF was sampled with 346 cm^2 funnels connected to 20 L plastic bottles. The TF sampled using bottles was manually weighed and the TF at the plot scale for each period was determined by averaging the available data from the bottles. Each collar around the trunk was connected to a 0.2 L tipping-bucket flow meter (handmade; cf. Shiraki et al., 2018) in each plot to measure SF because the high P at OEW causes large amount of SF. The SF measurements were sampled automatically as the time-of-tip by the event data logger (UA-003–64, Onset, MA). The number of bottles and flow meters used in each plot is shown in Table 1. Furthermore, the P losses by IC were calculated following Eq. (1). The IC data at Plots 1 and 4 from January 30, 2020 to December 28, 2021 and at Plot 3 from February 28, 2021 to December 28, 2021 were used for the analysis (the data from April 16, 2021 to August 19, 2021 were not included due to the uncertain values of P).

2.2. Canopy interception model

It may be expected that P is almost perfectly intercepted by a canopy in a light rainfall event and that the ratio of P and IC would reach β (terminal interception ratio) as P increases. Assuming that a single storm event does not exceed one day and that multiple storm events during a day can be combined as a single daily storm, the wet canopy evaporation by daily IC (mm day^{-1}) can be defined as zero when daily P is zero and asymptotically reaches a maximum value of the daily IC with increasing P, as given by the following equation (Linsley et al., 1949):

$$IC(P) = S_t\left\{1 - \exp\left(-\frac{P}{S_t}\right)\right\}, \quad (2)$$

where S_t is the maximum value of the daily IC, assumed to be the canopy storage capacity (mm). Considering $\frac{dIC}{dP} = \exp\left(-\frac{P}{S_t}\right)$, derived from Eq. (2), and $\lim_{P\to 0}\frac{dIC}{dP} = 1$ and $\lim_{P\to\infty}\frac{dIC}{dP} = \beta$ from the above expectation, we assumed a modification of $\frac{dIC}{dP}$ as follows:

$$\frac{dIC}{dP} = (1-\beta)\exp\left(-\frac{P}{S_t}\right) + \beta. \quad (3)$$

The integral of Eq. (3) gives the following equation:

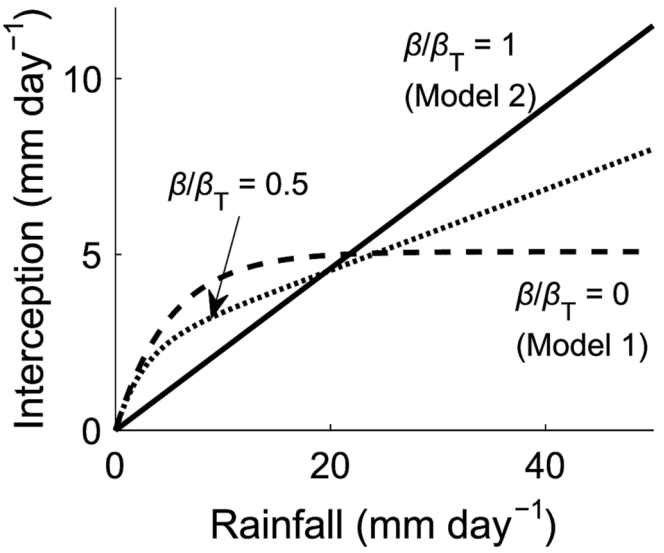

Fig. 2. Relationships between the daily interception and daily precipitation for different β/β_T, assuming the observed β_T at Plot 1 (0.23) and η_p calculated from the data observed from January 15, 2020 to December 31, 2021 (17.0 mm day^{-1}).

$$\mathrm{IC}(P) = (1-\beta)S_t\left\{1-\exp\left(-\frac{P}{S_t}\right)\right\}+\beta P. \tag{4}$$

The evaporation rate by IC should be controlled by P (mm day^{-1}). Moreover, an IC model linked to a stochastic representation of the P at an event can be used to describe the effects of the P regimes, such as frequent light rainfall and infrequent heavy rainfall events (e.g., de Groen and Savenije, 2006). The daily P is assumed to be an independent random variable, expressed by an exponential probability density function (see Rodriguez-Iturbe et al., 1999):

$$f(P) = \frac{1}{\eta_p}\exp\left(-\frac{P}{\eta_p}\right), \tag{5}$$

where η_p is the mean depth of rainfall events (mm day^{-1}). Note that $\mathrm{E}[P] = \eta_p$, where $\mathrm{E}[\cdot]$ is the mean value. Assuming $\mathrm{E}[\mathrm{IC}] = \beta_T\mathrm{E}[P] = \beta_T\eta_p$ (where β_T is the IC ratio over the total observation period) and the IC function of P (i.e., IC(P)), E[IC] can also be written as follows:

$$\mathrm{E}[\mathrm{IC}] = \int_0^\infty \mathrm{IC}(P)f(P)\mathrm{d}P = \beta_T\eta_p. \tag{6}$$

The S_t function of β can be derived by substituting Eqs. (4) and (5) for Eq. (6), resulting in the IC formulation as follows:

$$\mathrm{IC}(P) = \begin{cases} (1-\beta)\dfrac{\beta_T-\beta}{1-\beta_T}\eta_p\left\{1-\exp\left(-\dfrac{1-\beta_T}{\beta_T-\beta}\dfrac{P}{\eta_p}\right)\right\}+\beta P & \text{for } 0\le\dfrac{\beta}{\beta_T}<1 \\ \beta_T P & \text{for } \dfrac{\beta}{\beta_T}=1. \end{cases} \tag{7}$$

Here, β also represents a measure of the linearity of an increasing IC with the P and can vary between 0 (for the complete canopy storage saturation model, i.e., Model 1) and β_T (for the completely proportional model, i.e., Model 2); the canopy storage capacity control of the IC evaporation progressively weakens as β approaches β_T (i.e., $\frac{\beta}{\beta_T} = 1$). Fig. 2 shows the difference in the calculated daily IC as β changes.

2.3. Catchment water balance model

Given little bedrock drainage and intercatchment groundwater flow, Q can be expressed as the function of soil water storage, following the original TOPMODEL concept (Beven and Kirkby, 1979). In our previous study (Momiyama et al., 2021), we observed that in the studied catchment, the TOPMODEL, where the soil parameter representing the transmissivity (T_{max}) was zero, performed as well as the model considering the optimized T_{max}. In this case, we can use a lumped rainfall-runoff model, the tank model (Sugawara, 1972, 1995), compatible with the TOPMODEL to reproduce the daily Q from the studied catchment. The vertically integrated continuity equation describes the catchment water balance to compute the catchment average saturation deficit $\overline{D_s}$ (mm), given as follows:

$$\frac{d\overline{D_s}}{dt} = \mathrm{TR}+\mathrm{IC}+Q-P, \tag{8}$$

where t is time (day), and daily TR is canopy transpiration rate (mm day^{-1}). We assumed multiple discharges from a single tank would integrate into the daily Q (mm day^{-1}) as follows:

$$Q = \sum_{i=1}^{N}\max\{0, a_i(H-h_i)\}, \tag{9}$$

where N is the number of discharge holes in the tank, i identifies each discharge hole, a_i and h_i are fitting parameters, and H is the current water depth in the tank. Note that h_i represents the height of discharge hole i from the bottom of the tank. A comparison between TOPMODEL and Eq. (9) allows us to derive the following relationships:

$$a_i = \frac{k_t}{N}, \tag{10}$$

$$H = -\overline{D_s}+C, \tag{11}$$

and

$$h_i = m(\overline{\mathrm{TI}}-\mathrm{TI}_i)+C, \tag{12}$$

where k_t, m, $\overline{\mathrm{TI}}$, and TI_i are the TOPMODEL parameters, N is the number of grids in the digital elevation model of the studied catchment in the TOPMODEL, and C is a height reference to make H and h_i positive. The k_t is a time constant; m is a soil parameter replacing ϕ / f_s, where ϕ is soil porosity and f_s defines the decrease of saturated hydraulic conductivity with depth; and $\overline{\mathrm{TI}}$ and TI_i are the topographic indices TI, as the catchment average and the value at a given point i, respectively. TI is defined as $\ln(A/\tan\theta)$, where A is the contributing catchment area per unit contour length and θ is the local slope. The a_i is found to be a constant independent of i from Eq. (10).

To calculate the daily TR, we used the same TR model used by Momiyama et al. (2021). In general, the boundary conductance of conifers is sufficiently large, and Kumagai et al. (2008) confirmed that *Cr. japonica* canopies are aerodynamically well-coupled to the atmosphere. Hence, we used a modified McNaughton and Black (1973) expression to compute the daily TR given as follows:

$$\mathrm{TR} = 12\times 3600\times\frac{\rho_a c_p \mathrm{VPD}}{\rho_w\lambda\gamma}G_s, \tag{13}$$

in which

$$G_s = 4.30\times10^{-3}\overline{R_s}\times(1-5.78\times\ln\overline{\mathrm{VPD}}), \tag{14}$$

where ρ_a is the density of dry air (kg m^{-3}), c_p is the heat capacity of air (J kg^{-1} K^{-1}), ρ_w is the density of water (kg m^{-3}), λ is the latent heat of vaporization of water (J kg^{-1}), and γ is a psychrometric constant (Pa K^{-1}). The VPD used in Eq. (13) is the mean daytime value (Pa). The G_s is the monthly mean surface conductance (mm s^{-1}) expressed using a multiplicative-type function (Eq. 14) (e.g., Jarvis, 1976) where $\overline{R_s}$ and $\overline{\mathrm{VPD}}$ are monthly mean R_s (W m^{-2}) and VPD (kPa). Note that Eq. (14) is estimated using ET calculated from the short-term water balance method (Linsley et al., 1958; Suzuki, 1985), and IC is calculated assuming that $\beta_T = 0.184$ (see Momiyama et al., 2019, 2021).

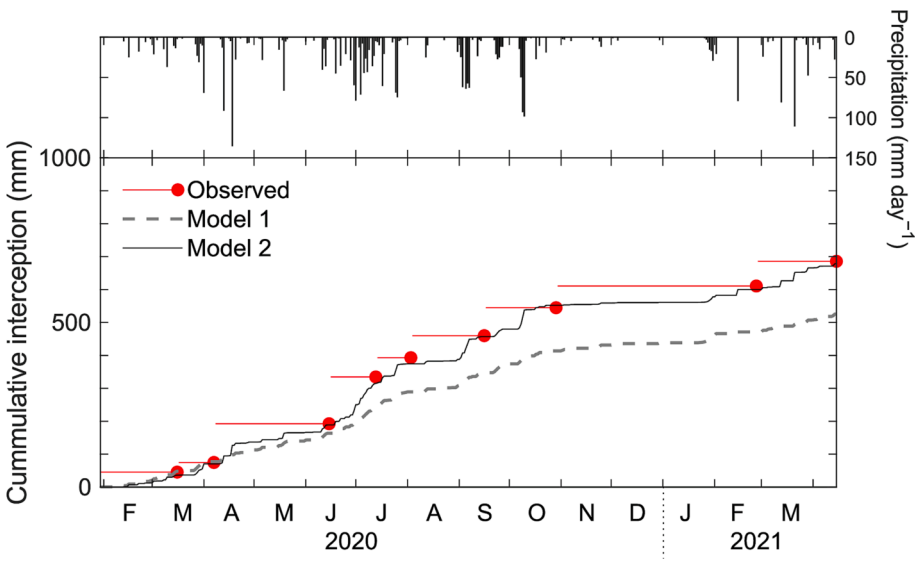

Fig. 3. Daily precipitation (upper panel) and observed and modeled cumulative interception (lower panel) in Plot 1 (Fig. 1). Red closed circles represent the observed cumulative interception until that point, and red horizontal lines denote the intervals of throughfall observation, that is, the periods of each interception observation. Broken and solid lines denote modeled values assuming the complete canopy storage saturation model ($\beta/\beta_T = 0$; Model 1) and the completely proportional model ($\beta/\beta_T = 1$; Model 2), respectively. For the modeling, we used $\beta_T = 0.23$ obtained from the observation in Plot 1. The results for January 30, 2020–April 15, 2021 have been shown because the data for April 16, 2021–August 19, 2021 were omitted from the analysis. (For interpretation of the references to colour in this figure legend, the reader is referred to the web version of this article.)

2.4. Model optimization

To evaluate the model fitness and obtain the optimized parameters (β_T [total interception ratio], β/β_T [β denotes terminal interception ratio], and m [water retention capacity of the catchment]) the TOPMODEL-based tank model was calibrated using various combination of β_T, β/β_T, and m values (0.03–0.25, 0–1, and 0.03–0.09 m at an interval of 0.001, 0.01 and 0.001 m, respectively) and comparing it with the 2010–2015 observational data. We used the Nash–Sutcliffe efficiency (Nash and Sutcliffe, 1970) criterion as an evaluation function for the optimization and performed two types of optimizations, given the importance of high and low streamflow (Criss and Winston, 2008; Pushpalatha et al., 2012): the ordinary Nash–Sutcliffe efficiency (NS) and the Nash–Sutcliffe efficiency with inverse Q values (NS_{inv}), given as follows:

$$NS = 1 - \frac{\sum_{j=1}^{n}\left(Q_{oj} - Q_{mj}\right)^2}{\sum_{j=1}^{n}\left(Q_{oj} - \overline{Q_{oj}}\right)^2}, \tag{15}$$

and

$$NS_{inv} = 1 - \frac{\sum_{j=1}^{n}\left(\frac{1}{Q_{oj}} - \frac{1}{Q_{mj}}\right)^2}{\sum_{j=1}^{n}\left(\frac{1}{Q_{oj}} - \overline{\left(\frac{1}{Q_{oj}}\right)}\right)^2}, \tag{16}$$

where n is the total number of time steps, subscript j denotes each time step, Q_o and Q_m are observed and simulated Q, respectively, and the overbar denotes the ensemble mean.

3. Results

3.1. Hydrological observations

The mean annual P for 2010–2015 was 3028 mm. Large rainfall events occurred during the rainy season from the middle of June to early July (668 ± 142 mm for June–July; mean ± SD) and the typhoon season from September to October (915 ± 200 mm). The mean annual Q for 2010–2015 was estimated to be 2261 mm when the missed data were replaced by the estimation using the model with NS-optimized parameters (the detailed optimization result will be shown later). The results of the IC observations at Plots 1, 3, and 4 (Fig. 1, Table 1) are shown in Table A1. The total P during the IC observation period (from January 30, 2020 to December 28, 2021, except for the period from April 16, 2021 to August 19, 2021) was 3765 mm, and TF, SF, and IC accounted for 61%–77%, 5%–20%, and 18%–23% of P, respectively.

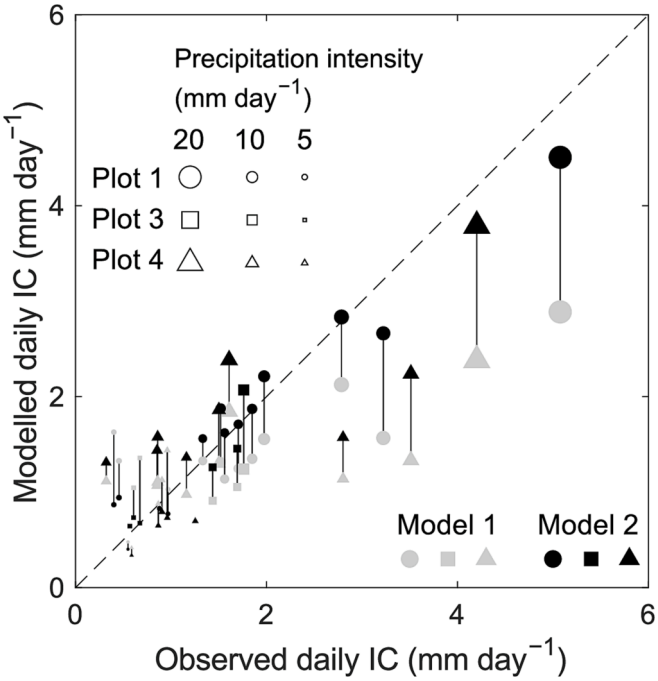

Fig. 4. Comparison between observed and modeled daily canopy interception (IC) from January 30, 2020, to December 28, 2021. The daily IC and precipitation intensity in this figure are obtained from the total observed (or modeled) IC (or precipitation) of the observation period divided by the days of the period. Circles, squares, and triangles denote values in Plots 1, 3, and 4, respectively. Gray and black symbols are the modeled values assuming the complete canopy storage saturation model ($\beta/\beta_T = 0$; Model 1) and the completely proportional model ($\beta/\beta_T = 1$; Model 2), respectively. Precipitation intensity is represented by the size of each symbol. The broken line shows a 1:1 line.

3.2. Comparisons between observed and modeled canopy interceptions

The observed IC in Plot 1 (Fig. 1), modeled IC estimated by the complete canopy storage saturation model ($\beta/\beta_T = 0$; Model 1), and the completely proportional model ($\beta/\beta_T = 1$; Model 2) were compared (Fig. 3). Model 2 reproduced the observed IC better than Model 1, and

Table 2
Parameters optimized using NS (Nash–Sutcliffe efficiency, Eq. 15) and NS_{inv} (Nash–Sutcliffe efficiency with inverse Q values, Eq. 16).

		Parameters		
Objective function	Value	β_T	β/β_T	m (m)
NS	0.830	0.133	1	0.063
NS_{inv}	0.763	0.093	1	0.046

*β_T denotes total interception ratio, β denotes terminal interception ratio, and m denotes water retention capacity of the catchment.

the difference in cumulative IC estimation mainly expanded during periods of high rainfall intensity (June–October 2020). Fig. 4 shows a further comparison between the observed and modeled IC. At a lower rainfall intensity, Model 1 and Model 2 show a minimal difference in performance. However, during high IC intensity, Model 1 underestimated IC. Note that during high IC intensity, Model 2 (an end-member) seems to be the nearest for the 1:1 line rather than the horizontal line between Models 1 and 2 (implying hybrid models [i.e., $0 < \beta/\beta_T < 1$]).

3.3. Optimization of the canopy interception model in the catchment water balance model

The IC model was incorporated into the catchment water balance

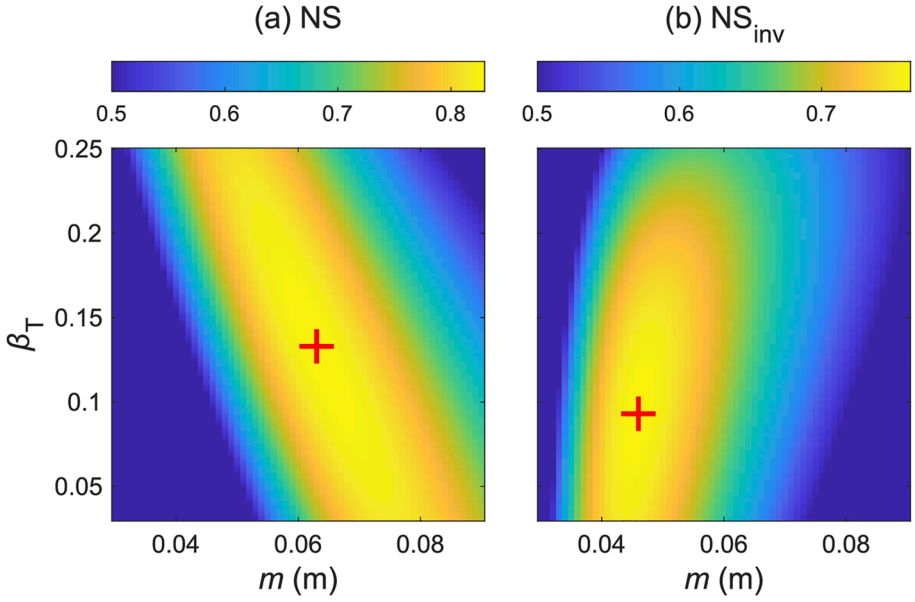

Fig. 5. (a) The ordinary Nash–Sutcliffe efficiency (NS) and (b) the Nash–Sutcliffe efficiency with inverse runoff values (NS_{inv}) with the two varying parameters of Model 2 ($\beta/\beta_T = 1$), that is, the catchment water retention capacity (m) and the total interception ratio (β_T). The crosses denote the points at maximum NS (0.830) and NS_{inv} (0.763), which are described in Table 2.

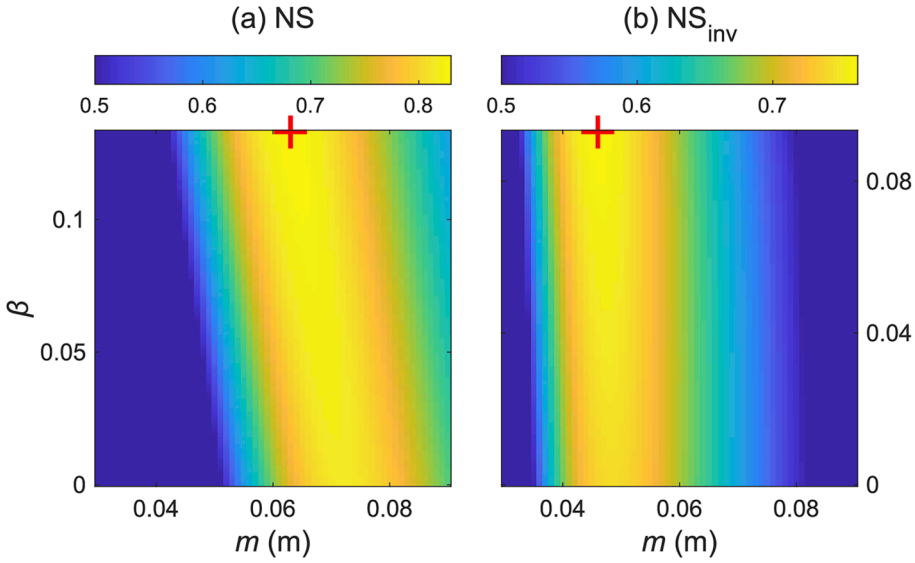

Fig. 6. (a) The ordinary Nash–Sutcliffe efficiency (NS) and (b) the Nash–Sutcliffe efficiency with inverse runoff values (NS_{inv}) with varying two model parameters (i.e., the catchment water retention capacity [m] and the terminal interception ratio [β] while fixing β_T). The crosses denote the points at maximum NS (0.830) and NS_{inv} (0.763) with $\beta_T = 0.133$ and 0.093, respectively (see also Table 2).

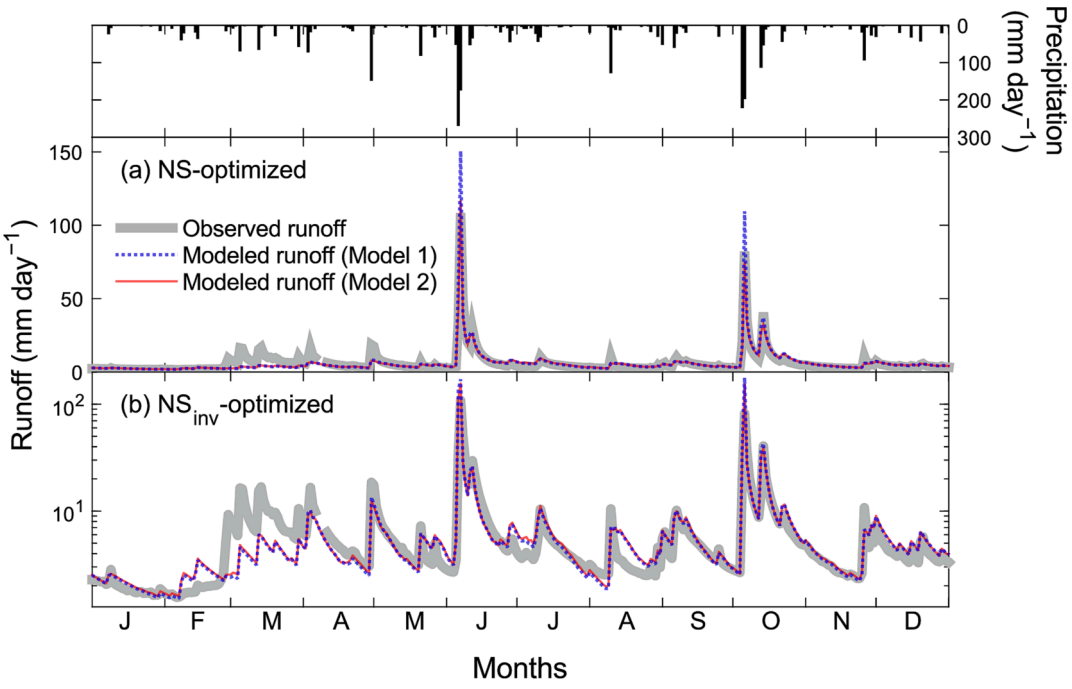

Fig. 7. Daily precipitation (upper panel) and observed and modeled daily runoff optimized using the ordinary Nash–Sutcliffe efficiency (NS) (a) and the Nash–Sutcliffe efficiency with inverse runoff values (NS_{inv}) (b) in the studied catchment in 2014. The optimized m and β_T shown in Table 2 are used ($m = 0.063$ m, $\beta_T = 0.133$ for NS, and $m = 0.046$ m, $\beta_T = 0.093$ for NS_{inv}). The models assumed the complete canopy storage saturation model ($\beta/\beta_T = 0$; Model 1) and the completely proportional model ($\beta/\beta_T = 1$; Model 2).

model, and the parameters were optimized to maximize objective functions (i.e., NS [Nash–Sutcliffe efficiency, Eq. 15] or NS_{inv} [Nash–Sutcliffe efficiency with inverse Q values, Eq. 16]) (Table 2). As expected from the above section, NS and NS_{inv} maxima were obtained at $\beta/\beta_T = 1$, or Model 2. Optimized β_T (total interception ratio) and m (water retention capacity of the catchment) were higher when optimized with NS ($\beta_T = 0.133$, $m = 0.063$ m) than NS_{inv} ($\beta_T = 0.093$, $m = 0.046$ m). The β_T estimated through optimization (Table 2, 0.09 and 0.13) were lower than those observed in the plots (Table A1, 0.18–0.23).

$\beta/\beta_T = 1$, or Model 2, was optimal in reproducing the observed IC and the rainfall-runoff processes using the catchment water balance model. Hence, assuming $\beta/\beta_T = 1$, we investigated the change in NS and NS_{inv} by altering β_T and m (Fig. 5). NS can be sufficiently high within the range $m = 0.06$–0.07 m by taking appropriate β_T, ranging from 0.1 to 0.2 (Fig. 5a). This shows that the combinations of their magnitudes, not the magnitude of each β_T and m, are important for reproducing high flows. NS_{inv} is high enough in the case of $m \sim 0.05$ m, and β_T has little effect when β_T is within the wide range of $\beta_T = 0.05$–0.15 (Fig. 5b). This means that determining m is of paramount importance for reproducing low flows while determining β_T is of relatively low priority.

Accepting that NS and NS_{inv} are maximized at $\beta/\beta_T = 1$, we examined the effect of changes in β (terminal interception ratio) on NS and NS_{inv} when fixing β_T (Fig. 6; $\beta_T = 0.133$ for NS and 0.093 for NS_{inv}, according to the optimization result shown in Table 2). NS was sufficiently high over a wide range of β (0.05–β_T) when $m \sim 0.065$ m (Fig. 6a). Furthermore, NS_{inv} was sufficiently high over a wide range of β (0.04–β_T) when $m \sim 0.045$ m (Fig. 6b). These results show that the observed daily Q can be reproduced sufficiently regardless of β if m is properly optimized.

Moreover, the completely proportional model ($\beta/\beta_T = 1$; Model 2) most accurately reproduced the observed IC and observed daily Q. This indicates that the most appropriate m in the catchment water balance model can be determined using Model 2 ($m = 0.063$ m and 0.046 m for NS and NS_{inv} cases, respectively) at OEW. In addition, it can be inferred that enormous daily P is intercepted by the higher β_T and optimally buffered by the higher m when focusing on reproducing high flow, since the optimized m is higher when optimized with the NS than the NS_{inv} (Table 2). Here, we examined how the complete canopy storage saturation model ($\beta/\beta_T = 0$; Model 1) and the completely proportional model ($\beta/\beta_T = 1$; Model 2) reproduce high flow (targeted by NS) and low flow (targeted by NS_{inv}) under the condition that the catchment soil water retention capacity (m) is preliminarily determined by NS or NS_{inv} (Figs. 7 and 8).

The modeled hydrograph shows that applying Model 1 induces a much larger high-flow estimation than when Model 2 is applied (Fig. 7a). Conversely, there was little difference in performance in reproducing low flow between Models 1 and 2 (Fig. 7b). Fig. 8 further compares flow duration curves of modeled Q assuming Models 1 and 2 against flow duration curves of 2010–2015 observational data under the high- and low-flow conditions. Changing Model 2 to Model 1 affects high flows and makes them higher (Fig. 8a), while no difference was observed between the performance of Model 1 and 2 at low flows (Fig. 8b).

4. Discussion and conclusion

4.1. Validity of the interception model

Under the period with low P intensity, the complete canopy storage saturation model ($\beta/\beta_T = 0$; Model 1), which can reflect the characteristics of IC that much of the P is intercepted (e.g., Sun et al., 2015), performed similarly to the completely proportional model with P ($\beta/\beta_T = 1$; Model 2) (Fig. 4). Model 1 constantly underestimates IC during heavy rainfall (Figs. 3 and 4). Note that the total IC calculated by Model 2 always matches the total observed IC because Model 2 uses the ratio of IC to P throughout the observation period (β_T) as the slope of the linear function. Errors in Model 1 continue to accumulate when applying the same β_T and this induces a huge underestimation of total IC, an important component of the annual water budget.

The IC underestimation of Model 1 during heavy rainfall indicates that some mechanisms cannot be described using the mechanism represented by the model including the canopy storage term (Eq. 7). The findings on the mechanism of such IC during heavy rainfall may help us

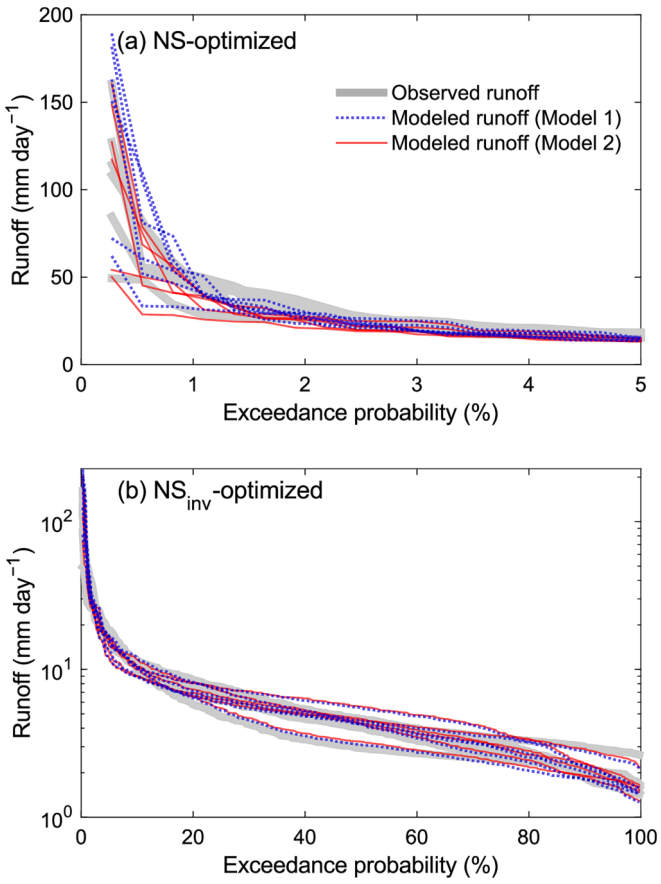

Fig. 8. Flow duration curves made of observed and modeled daily runoff optimized using (a) the ordinary Nash–Sutcliffe efficiency (NS) and (b) the Nash–Sutcliffe efficiency with inverse runoff values (NS_{inv}) in the studied catchment from 2010 to 2015. The optimized m and β_T shown in Table 2 are used ($m = 0.063$ m, $\beta_T = 0.133$ for NS, and $m = 0.046$ m, $\beta_T = 0.093$ for NS_{inv}). The models assumed the complete canopy storage saturation model ($\beta/\beta_T = 0$; Model 1) and the completely proportional model ($\beta/\beta_T = 1$; Model 2).

improve IC models. One possible explanation is "splash droplet evaporation" (Dunkerley, 2009; Murakami, 2006). The canopy changes the distribution of drop size (Levia et al., 2017; Nanko et al., 2022; Zore et al., 2022). Also, some raindrops impacting the canopy surface become splashes (Roth-Nebelsick et al., 2022), which have a relatively large surface area compared to their small volume that may be subject to greater evaporation from their surfaces (Murakami, 2006).

When considering the water storage of vegetation, the contribution of the bark on stems as well as foliage and branch is important (Iida et al., 2017; Levia and Herwitz, 2005). Since S_t (canopy storage capacity) is obtained from only β_T (total IC rate) and η_p (P characteristics) in our model (Eq. 7), S_t in our study should include such bark storage. Based on a set of laboratory experiments, Iida et al. (2017) estimated stand-scale water storage capacity by the tree surface, including leaf and bark, in a Japanese conifer plantation with $\beta_T = 0.199$ and $\eta_p = 22.3$ mm event^{-1} to be 4.4–7.2 mm. In our model, canopy water storage capacity was estimated to be 5.5 mm under $\beta/\beta_T = 0$ (Model 1; cf. Eq. 7) conditions, which is within the range reported by Iida et al. (2017). Iida et al. (2017) showed that the water storage capacity of the stand was similar to the maximum IC value measured, which is similar to our assumption of Model 1. Although this is against our result (Figs. 3 and 4), our model has the potential to be a useful tool for further investigations on the water storage of vegetation.

In our model, P characteristics are represented by only an exponential probability density function of daily P when rainfall occurs. The frequency and amount of each rainfall event were not considered. In particular, Model 2 cannot reflect the change in P characteristics, which can be altered due to climate change. Thus, Model 2 would underestimate the actual IC if light rainfall events that were almost perfectly intercepted by the canopy became more frequent (see Kumagai et al., 2004). Hence, our result that Model 2 is the best model of IC still needs to be discussed based on more data.

4.2. Effects of canopy interception on catchment runoff

The results showed that it is more important to accurately estimate the water retention capacity of catchment (m) than the assumption of the IC model regarding the estimation of daily Q using the catchment water balance model (Figs. 5 and 6). Since the observed P is 3028 mm year^{-1} at OEW, β_T (total interception ratio) difference by 0.1 results in an approximately 300 mm year^{-1} difference in IC and Q. However, NS and NS_{inv} become as high as the optimized value at a wide range of β_T (Fig. 5). Similar to previous studies showing that simple potential ET models work as well as precise potential ET (evapotranspiration) models (e.g., Oudin et al., 2005b), the catchment water balance model would act as a filter that mitigates the impact of change in IC.

Our results also showed the parameter insensitivity of β_T or β (terminal interception ratio) while focusing on NS_{inv} (Fig. 5b and 6b) and parameter interaction between m and β_T (Fig. 5a) or β (Fig. 6a) while focusing on NS. They seem to be examples of equifinality (Beven, 1993). The result considering high flow (Fig. 5a and 6a) showed that high/low β or β_T in the IC model induces underestimation/overestimation of the high flow due to the lower/higher P input for catchment, and the misestimation of IC modeling was compensated by lower/higher m in order to satisfy objective functions, as Savenije (2004) instructed. Considering the parameter insensitivity/interaction shown in Fig. 5 and the discrepancy between observed β_T (Table A1) and optimized β_T (Table 2), a wrong β_T may be obtained from an optimization using daily Q. Although the IC mechanism during storms is still uncertain, the subsurface stormflow mechanism is still very hard to model and validate (see Chifflard et al., 2019). Thus, a practical way to model rainfall-runoff processes may be to identify the IC mechanism from intensive observations and then model the runoff generation mechanism from the inference using the observed daily Q.

Since the completely proportional model ($\beta/\beta_T = 1$; Model 2) reproduced the observed IC well, and this result was also supported by the optimization of the catchment water balance model, it would be reasonable to consider the runoff processes (e.g., the determination of m) under the assumption of Model 2, at least in our study site. Although β_T, the only parameter needed in Model 2, takes various values depending on forest conditions (Carlyle-Moses and Gash, 2011), it has been observed in various vegetation types globally (Yue et al., 2021). One of the main assertions in this study is that catchment water balance models incorporating Model 2 would be a strong tool to predict the impact of forest management on high flow by associating β_T with the forest status, for example, species, LAI, or stand density (Komatsu, 2020; Komatsu et al., 2007).

In this paper, the water retention capacity of catchment (m) was determined through the incorporation of Model 2, and the effect of differences in the IC model assumption on the rainfall-runoff process was investigated. There was no significant difference between selecting Model 1 or Model 2 for the IC model in the low-flow and intermediate-flow domains (Fig. 7b and 8b). However, a large difference was induced by the selection of Model 1 and Model 2 in a high-flow domain (Fig. 7a and 8a). The low estimated IC during heavy rain by Model 1 led to an increase of the effective rainwater input, which increased the high flow. This shows that the high flow cannot be adequately represented without incorporating an IC model that can represent its mechanism during heavy rain as a submodel of catchment water balance models. This may be obvious because IC occurs before rainfall reaches the soil and therefore precedes rainfall-runoff processes within catchments. Yokoo and Sivapalan (2011) indicated that ET can control low flow; however,

Table A1
Throughfall (TF), stem flow (SF), and interception (IC) observed at Plots 1, 3, and 4.

Period	P (mm)[a]	Plot 1			Plot 3			Plot 4		
		TF (mm)	SF (mm)	IC (mm)	TF (mm)	SF (mm)	IC (mm)	TF (mm)	SF (mm)	IC (mm)
30 Jan 2020–16 Mar 2020	161.3	105.5	10.2	45.5				93.4	27.1	40.7
17 Mar 2020–7 Apr 2020	152.5	110.9	12.2	29.3				103.9	41.5	7.1
8 Apr 2020–15 Jun 2020	524.0	374.5	31.8	117.6				325.2	139.9	58.9
16 Jun 2020–13 Jul 2020	560.2	396.3	21.9	142.1				355.0	87.6	117.7
14 Jul 2020–3 Aug 2020	264.3	200.0	5.8	58.5				172.6	57.9	33.8
4 Aug 2020–16 Sep 2020	366.6	274.5	25.2	66.9				244.1	84.6	37.9
17 Sep 2020–29 Oct 2020	422.6	293.4	44.2	84.9				229.7	128.3	64.6
30 Oct 2020–26 Feb 2021	214.5	134.4	14.1	65.9				116.6	27.4	70.5
27 Feb 2021–15 Apr 2021	345.7	234.1	36.6	74.9	259.7	17.0	69.0	216.5	73.4	55.8
20 Aug 2021–15 Sep 2021	113.0	91.0	9.7	12.3	92.8	3.8	16.4	71.5	17.1	24.4
16 Sep 2021–5 Oct 2021	236.5	147.7	24.3	64.5	189.2	12.0	35.2	131.9	34.3	70.2
6 Oct 2021–21 Oct 2021	61.7	51.7	3.6	6.4	49.1	1.8	10.8	41.9	4.5	15.4
22 Oct 2021–10 Nov 2021	166.2	113.7	15.5	37.0	122.6	9.8	33.9	98.7	11.4	56.0
11 Nov 2021–28 Dec 2021	176.4	110.3	23.9	42.2	137.7	11.5	27.3	88.7	27.5	60.2
Total	3765.4	2638.2	279.2	848.1	851.1	55.9	192.5	2289.7	762.7	713.1
(Ratio to P)[a]		(0.70)	(0.07)	(0.23)	(0.77)	(0.05)	(0.18)	(0.61)	(0.20)	(0.19)

[a] P denotes precipitation measured at the weather station (Fig. 1).

the effect of ET on low flow may be caused by TR (transpiration) or EF (forest floor evaporation). Our study showed that IC, which affects high flow, can play a different role compared to TR and EF. Although there is an uncertainty of calculated value at extreme rainfall events (Page et al., 2020), we can infer that forest management altering IC has the potential to control floods.

In this study, we did not elaborate on the effect on the IC of rainfall regimes, that is, the mean depth of rainfall events, η_p. However, Eq. (7) may be applied to enhance our understanding of IC change due to climate change. Global warming will increase the frequency of heavy rainfall (Pendergrass and Knutti, 2018), and this can result in an increased η_p. For example, supposing that the preceding study with lower η_p and the follow-up study with higher η_p reported the same β_T and β, IC for certain P is estimated to be larger at the condition of the follow-up study according to Eq. (7) unless $\beta/\beta_T = 1$. This is because canopy storage capacity (S_t) would be larger for the follow-up condition, and if η_p were the same as in the preceding one, β_T would have been even larger. Furthermore, if β_T and β are represented by forest condition and present and future η_p are available, the skill and technology shown in this study will be a strong tool to project how the change in forest condition (e.g., forest management and forest disturbances) or global and local climate change can change high flow from forested headwater.

To answer the questions posed initially, we can state that the completely proportional model (Model 2) can reproduce the observed IC and runoff efficiently, and that IC model selection affects high flow rather than low flow. The results of this study also indicate that increasing IC can reduce flood discharge. Therefore, IC changes due to forest management has the potential to contribute to nature-based solutions (Cohen-Shacham et al., 2016) with regard to flood risk management.

CRediT authorship contribution statement

Hiroki Momiyama: Conceptualization, Methodology, Software, Formal analysis, Writing – original draft, Visualization, Funding acquisition. **Tomo'omi Kumagai:** Conceptualization, Writing – review & editing, Supervision, Project administration, Funding acquisition. **Naoya Fujime:** Investigation, Data curation, Writing – review & editing. **Tomohiro Egusa:** Investigation, Data curation, Writing – review & editing. **Takanori Shimizu:** Writing – review & editing, Supervision, Project administration, Funding acquisition.

Declaration of Competing Interest

The authors declare that they have no known competing financial interests or personal relationships that could have appeared to influence the work reported in this paper.

Data availability

Data will be made available on request.

Acknowledgments

The funding for this work was provided by the Kanagawa Prefectural Government, Japan, as part of the project on "Forest, soil, and water resource conservation in the western Kanagawa reservoir area," Research grant #202210 of the Forestry and Forest Products Research Institute (FFPRI), and "Global Environmental Research Coordination System (MAFF1942)" from Ministry of the Environment of Japan. The authors thank the staff of the Kanagawa Prefectural Government for logistical support in conducting observations throughout the Oborasawa Experimental Watershed (OEW), Members of Forest Biogeosciences Lab (The University of Tokyo) for logistical support, and Dr. Shin'ichi Iida (FFPRI) for his assistance with manuscript preparation. H. M. is grateful to the Support for Pioneering Research Initiated by the Next Generation (SPRING) of Japan Science and Technology Agency (JST), Grant Number JPMJSP2108.

Appendix A

References

Andréassian, V., 2004. Waters and forests: From historical controversy to scientific debate. J. Hydrol. 291, 1–27. https://doi.org/10.1016/j.jhydrol.2003.12.015.
Bai, P., Liu, X., Yang, T., Li, F., Liang, K., Hu, S., Liu, C., 2016. Assessment of the influences of different potential evapotranspiration inputs on the performance of monthly hydrological models under different climatic conditions. J. Hydrometeorol. 17, 2259–2274. https://doi.org/10.1175/JHM-D-15-0202.1.
Beven, K., 1993. Prophecy, reality and uncertainty in distributed hydrological modelling. Adv. Water Resour. 16, 41–51. https://doi.org/10.1016/0309-1708(93)90028-E.
Beven, K., Kirkby, M.J., 1979. A physically based, variable contributing area model of basin hydrology. Hydrol. Sci. Bull. 24, 43–69. https://doi.org/10.1080/02626667909491834.
Bosch, J.M., Hewlett, J.D., 1982. A review of catchment experiments to determine the effect of vegetation changes on water yield and evapotranspiration. J. Hydrol. 55, 3–23. https://doi.org/10.1016/0022-1694(82)90117-2.
Calder, I.R., 2007. Forests and water—ensuring forest benefits outweigh water costs. For. Ecol. Manage. 251, 110–120. https://doi.org/10.1016/j.foreco.2007.06.015.
Carlyle-Moses, D.E., Gash, J.H.C., 2011. Rainfall Interception Loss by Forest Canopies. In: Levia, D.F., Carlyle-Moses, D., Tanaka, T. (Eds.), Forest Hydrology and Biogeochemistry: Synthesis of Past Research and Future Directions. Springer,

Netherlands, Dordrecht, pp. 407–423. https://doi.org/10.1007/978-94-007-1363-5_20.
Chifflard, P., Blume, T., Maerker, K., Hopp, L., van Meerveld, I., Graef, T., Gronz, O., Hartmann, A., Kohl, B., Martini, E., Reinhardt-Imjela, C., Reiss, M., Rinderer, M., Achleitner, S., 2019. How can we model subsurface stormflow at the catchment scale if we cannot measure it? Hydrol. Process. 33, 1378–1385. https://doi.org/10.1002/hyp.13407.
Cohen-Shacham, E., Walters, G., Maginnis, S., Janzen, C. (Eds.), 2016. Nature-based Solutions to Address Global Societal Challenges. International Union for Conservation of Nature, Gland. https://doi.org/10.2305/IUCN.CH.2016.13.en.
Criss, R.E., Winston, W.E., 2008. Do Nash values have value? Discussion and alternate proposals. Hydrol. Process. 22, 2723–2725. https://doi.org/10.1002/hyp.7072.
de Groen, M.M., Savenije, H.H.G., 2006. A monthly interception equation based on the statistical characteristics of daily rainfall. Water Resour. Res. 42, W12417. https://doi.org/10.1029/2006WR005013.
Delzon, S., Loustau, D., 2005. Age-related decline in stand water use: sap flow and transpiration in a pine forest chronosequence. Agric. For. Meteorol. 129, 105–119. https://doi.org/10.1016/j.agrformet.2005.01.002.
Dunkerley, D.L., 2009. Evaporation of impact water droplets in interception processes: historical precedence of the hypothesis and a brief literature overview. J. Hydrol. 376, 599–604. https://doi.org/10.1016/j.jhydrol.2009.08.004.
Egusa, T., Oda, T., Sato, T., Kumagai, T., 2021. Estimation of sub-annual inter-catchment groundwater flow using short-term water balance method. Hydrol. Process. 35, e14368 https://doi.org/10.1002/hyp.14368.
Ellison, D., Morris, C.E., Locatelli, B., Sheil, D., Cohen, J., Murdiyarso, D., Gutierrez, V., van Noordwijk, M., Creed, I.F., Pokorny, J., Gaveau, D., Spracklen, D.V., Tobella, A. B., Ilstedt, U., Teuling, A.J., Gebrehiwot, S.G., Sands, D.C., Muys, B., Verbist, B., Springgay, E., Sugandi, Y., Sullivan, C.A., 2017. Trees, forests and water: cool insights for a hot world. Glob. Environ. Chang. 43, 51–61. https://doi.org/10.1016/j.gloenvcha.2017.01.002.
Fan, J., Oestergaard, K.T., Guyot, A., Lockington, D.A., 2014. Measuring and modeling rainfall interception losses by a native Banksia woodland and an exotic pine plantation in subtropical coastal Australia. J. Hydrol. 515, 156–165. https://doi.org/10.1016/j.jhydrol.2014.04.066.
Fenicia, F., Savenije, H.H.G., Matgen, P., Pfister, L., 2008. Understanding catchment behavior through stepwise model concept improvement. Water Resour. Res. 44, W01402. https://doi.org/10.1029/2006WR005563.
Gash, J.H.C., 1979. An analytical model of rainfall interception by forests. Q. J. R. Meteorol. Soc. 105, 43–55. https://doi.org/10.1002/qj.49710544304.
Ghimire, C.P., Bruijnzeel, L.A., Lubczynski, M.W., Bonell, M., 2012. Rainfall interception by natural and planted forests in the Middle Mountains of Central Nepal. J. Hydrol. 475, 270–280. https://doi.org/10.1016/j.jhydrol.2012.09.051.
Good, S.P., Noone, D., Bowen, G., 2015. Hydrologic connectivity constrains partitioning of global terrestrial water fluxes. Science 349, 175–177. https://doi.org/10.1126/science.aaa5931.
Grunicke, S., Queck, R., Bernhofer, C., 2020. Long-term investigation of forest canopy rainfall interception for a spruce stand. Agric. For. Meteorol. 292–293, 108125 https://doi.org/10.1016/j.agrformet.2020.108125.
Guswa, A.J., Tetzlaff, D., Selker, J.S., Carlyle-Moses, D.E., Boyer, E.W., Bruen, M., Cayuela, C., Creed, I.F., van de Giesen, N., Grasso, D., Hannah, D.M., Hudson, J.E., Hudson, S.A., Iida, S., Jackson, R.B., Katul, G.G., Kumagai, T., Llorens, P., Lopes Ribeiro, F., Michalzik, B., Nanko, K., Oster, C., Pataki, D.E., Peters, C.A., Rinaldo, A., Sanchez Carretero, D., Trifunovic, B., Zalewski, M., Haagsma, M., Levia, D.F., 2020. Advancing ecohydrology in the 21st century: a convergence of opportunities. Ecohydrol. 13, e2208. https://doi.org/10.1002/eco.2208.
Iida, S., Levia, D.F., Shimizu, A., Shimizu, T., Tamai, K., Nobuhiro, T., Kabeya, N., Noguchi, S., Sawano, S., Araki, M., 2017. Intrastorm scale rainfall interception dynamics in a mature coniferous forest stand. J. Hydrol. 548, 770–783. https://doi.org/10.1016/j.jhydrol.2017.03.009.
IPCC, 2021. Summary for Policymakers, in: Masson-Delmotte, V., Zhai, P., Pirani, A., Connors, S.L., Péan, C., Berger, S., Caud, N., Chen, Y., Goldfarb, L., Gomis, M.I., Huang, M., Leitzell, K., Lonnoy, E., Matthews, J.B.R., Maycock, T.K., Waterfield, T., Yelekçi, O., Yu, R., Zhou, B. (Eds.), Climate Change 2021: The Physical Science Basis. Contribution of Working Group I to the Sixth Assessment Report of the Intergovernmental Panel on Climate Change. Cambridge University Press, Cambridge, pp. 3–32.
Jarvis, P.G., 1976. The interpretation of the variations in leaf water potential and stomatal conductance found in canopies in the field. Philos. Trans. R. Soc. B Biol. Sci. 273, 593–610. https://doi.org/10.1098/rstb.1976.0035.
Komatsu, H., 2020. Modeling evapotranspiration changes with managing Japanese cedar and cypress plantations. For. Ecol. Manage. 475, 118395 https://doi.org/10.1016/j.foreco.2020.118395.
Komatsu, H., Kume, T., 2020. Modeling of evapotranspiration changes with forest management practices: a genealogical review. J. Hydrol. 585, 124835 https://doi.org/10.1016/j.jhydrol.2020.124835.
Komatsu, H., Tanaka, N., Kume, T., 2007. Do coniferous forests evaporate more water than broad-leaved forests in Japan? J. Hydrol. 336, 361–375. https://doi.org/10.1016/j.jhydrol.2007.01.009.
Kumagai, T., Katul, G.G., Saitoh, T.M., Sato, Y., Manfroi, O.J., Morooka, T., Ichie, T., Kuraji, K., Suzuki, M., Porporato, A., 2004. Water cycling in a Bornean tropical rain forest under current and projected precipitation scenarios. Water Resour. Res. 40, W01104. https://doi.org/10.1029/2003WR002226.
Kumagai, T., Tateishi, M., Shimizu, T., Otsuki, K., 2008. Transpiration and canopy conductance at two slope positions in a Japanese cedar forest watershed. Agric. For. Meteorol. 148, 1444–1455. https://doi.org/10.1016/J.AGRFORMET.2008.04.010.
Kumagai, T., Tateishi, M., Miyazawa, Y., Kobayashi, M., Yoshifuji, N., Komatsu, H., Shimizu, T., 2014. Estimation of annual forest evapotranspiration from a coniferous plantation watershed in Japan (1): water use components in Japanese cedar stands. J. Hydrol. 508, 66–76. https://doi.org/10.1016/j.jhydrol.2013.10.047.
Levia, D.F., Herwitz, S.R., 2005. Interspecific variation of bark water storage capacity of three deciduous tree species in relation to stemflow yield and solute flux to forest soils. Catena 64, 117–137. https://doi.org/10.1016/j.catena.2005.08.001.
Levia, D.F., Hudson, S.A., Llorens, P., Nanko, K., 2017. Throughfall drop size distributions: a review and prospectus for future research. WIREs Water 4, e1225. https://doi.org/10.1002/wat2.1225.
Linsley, R.K.J., Kohler, M.A., Paulhus, J.L.H., 1949. Applied Hydrology. McGraw-Hill, New York.
Linsley, R.K., Kohler, M.A., Paulhus, J.L.H., 1958. Hydrology for engineers. McGraw-Hill, New York.
McNaughton, K.G., Black, T.A., 1973. A study of evapotranspiration from a douglas fir forest using the energy balance approach. Water Resour. Res. 9, 1579–1590. https://doi.org/10.1029/WR009i006p01579.
Momiyama, H., Kumagai, T., Egusa, T., 2019. Reproducing monthly evapotranspiration from a coniferous plantation watershed in Japan. J. For. Res. 24, 197–200. https://doi.org/10.1080/13416979.2019.1604606.
Momiyama, H., Kumagai, T., Egusa, T., 2021. Model analysis of forest thinning impacts on the water resources during hydrological drought periods. For. Ecol. Manage. 499, 119593 https://doi.org/10.1016/j.foreco.2021.119593.
Murakami, S., 2006. A proposal for a new forest canopy interception mechanism: splash droplet evaporation. J. Hydrol. 319, 72–82. https://doi.org/10.1016/j.jhydrol.2005.07.002.
Murakami, S., 2021. Water and energy balance of canopy interception as evidence of splash droplet evaporation hypothesis. Hydrol. Sci. J. 66, 1248–1264. https://doi.org/10.1080/02626667.2021.1924378.
Muzylo, A., Llorens, P., Valente, F., Keizer, J.J., Domingo, F., Gash, J.H.C., 2009. A review of rainfall interception modelling. J. Hydrol. 370, 191–206. https://doi.org/10.1016/j.jhydrol.2009.02.058.
Nanko, K., Onda, Y., Kato, H., Gomi, T., 2016. Immediate change in throughfall spatial distribution and canopy water balance after heavy thinning in a dense mature Japanese cypress plantation. Ecohydrol. 9, 300–314. https://doi.org/10.1002/eco.1636.
Nanko, K., Keim, R.F., Hudson, S.A., Levia, D.F., 2022. Throughfall drop sizes suggest canopy flowpaths vary by phenophase. J. Hydrol. 612, 128144 https://doi.org/10.1016/j.jhydrol.2022.128144.
Nash, J.E., Sutcliffe, J.V., 1970. River flow forecasting through conceptual models part I — a discussion of principles. J. Hydrol. 10, 282–290. https://doi.org/10.1016/0022-1694(70)90255-6.
Oda, T., Suzuki, M., Egusa, T., Uchiyama, Y., 2013. Effect of bedrock flow on catchment rainfall-runoff characteristics and the water balance in forested catchments in Tanzawa mountains. Japan. Hydrol. Process. 27, 3864–3872. https://doi.org/10.1002/hyp.9497.
Oren, R., Ewers, B.E., Todd, P., Phillips, N., Katul, G., 1998. Water balance delineates the soil layer in which moisture affects canopy conductance. Ecol. Appl. 8, 990–1002. https://doi.org/10.2307/2640956.
Oudin, L., Hervieu, F., Michel, C., Perrin, C., Andréassian, V., Anctil, F., Loumagne, C., 2005a. Which potential evapotranspiration input for a lumped rainfall-runoff model? Part 2—towards a simple and efficient potential evapotranspiration model for rainfall-runoff modelling. J. Hydrol. 303, 290–306. https://doi.org/10.1016/j.jhydrol.2004.08.026.
Oudin, L., Michel, C., Anctil, F., 2005b. Which potential evapotranspiration input for a lumped rainfall-runoff model? Part 1—can rainfall-runoff models effectively handle detailed potential evapotranspiration inputs? J. Hydrol. 303, 275–289. https://doi.org/10.1016/j.jhydrol.2004.08.025.
Page, T., Chappell, N.A., Beven, K.J., Hankin, B., Kretzschmar, A., 2020. Assessing the significance of wet-canopy evaporation from forests during extreme rainfall events for flood mitigation in mountainous regions of the United Kingdom. Hydrol. Process. 34, 4740–4754. https://doi.org/10.1002/hyp.13895.
Pendergrass, A.G., Knutti, R., 2018. The uneven nature of daily precipitation and its change. Geophys. Res. Lett. 45, 11980–11988. https://doi.org/10.1029/2018GL080298.
Pushpalatha, R., Perrin, C., Le Moine, N., Andréassian, V., 2012. A review of efficiency criteria suitable for evaluating low-flow simulations. J. Hydrol. 420–421, 171–182. https://doi.org/10.1016/j.jhydrol.2011.11.055.
Roberts, J., 1983. Forest transpiration: a conservative hydrological process? J. Hydrol. 66, 133–141. https://doi.org/10.1016/0022-1694(83)90181-6.
Rodriguez-Iturbe, I., Porporato, A., Ridolfi, L., Isham, V., Coxi, D.R., 1999. Probabilistic modelling of water balance at a point: the role of climate, soil and vegetation. Proc. R. Soc. Lond. Ser. A Math. Phys. Eng. Sci. 455, 3789–3805. https://doi.org/10.1098/rspa.1999.0477.
Roth-Nebelsick, A., Konrad, W., Ebner, M., Miranda, T., Thielen, S., Nebelsick, J.H., 2022. When rain collides with plants—patterns and forces of drop impact and how leaves respond to them. J. Exp. Bot. 73, 1155–1175. https://doi.org/10.1093/jxb/erac004.
Rutter, A.J., Kershaw, K.A., Robins, P.C., Morton, A.J., 1971. A predictive model of rainfall interception in forests, 1. Derivation of the model from observations in a plantation of Corsican pine. Agric. Meteorol. 9, 367–384. https://doi.org/10.1016/0002-1571(71)90034-3.
Savenije, H.H.G., 2004. The importance of interception and why we should delete the term evapotranspiration from our vocabulary. Hydrol. Process. 18, 1507–1511. https://doi.org/10.1002/hyp.5563.

Shinohara, Y., Levia, D.F., Komatsu, H., Nogata, M., Otsuki, K., 2015. Comparative modeling of the effects of intensive thinning on canopy interception loss in a Japanese cedar (*Cryptomeria japonica* D. Don) forest of western Japan. Agric. For. Meteorol. 214–215, 148–156. https://doi.org/10.1016/j.agrformet.2015.08.257.

Shiraki, K., Sun, J., Kagami, S., Nagai, K., Yokoyama, Y., Koyama, Y., Negi, K., Matsumoto, E., Kawase, S., 2018. Accuracy of low-cost flow meters for stemflow observation including handmade tipping buckets flow meter. J. Jpn. Soc. Hydrol. Water Resour. 31, 380–392. https://doi.org/10.3178/jjshwr.31.380 (in Japanese with English abstract).

Sugawara, M., 1972. Method of rainfall-runoff analysis. Kyoritsu Shuppan, Tokyo (in Japanese).

Sugawara, M., 1995. Tank Model. In: Singh, V.P. (Ed.), Computer Models of Watershed Hydrology. Water Resource Publications, Colorado, pp. 165–214.

Sun, G., Hallema, D., Asbjornsen, H., 2017. Ecohydrological processes and ecosystem services in the Anthropocene: a review. Ecol. Process. 6, 35. https://doi.org/10.1186/s13717-017-0104-6.

Sun, X., Onda, Y., Kato, H., Gomi, T., Komatsu, H., 2015. Effect of strip thinning on rainfall interception in a Japanese cypress plantation. J. Hydrol. 525, 607–618. https://doi.org/10.1016/j.jhydrol.2015.04.023.

Suzuki, M., 1985. Evapotranspiration estimates of forested watersheds in Japan using the short-time period water-budget method. J. Jpn For. Soc. 67, 115–125. https://doi.org/10.11519/jjfs1953.67.4_115 (in Japanese with English abstract).

Takahashi, M., Giambelluca, T.W., Mudd, R.G., DeLay, J.K., Nullet, M.A., Asner, G.P., 2011. Rainfall partitioning and cloud water interception in native forest and invaded forest in Hawai'i Volcanoes National Park. Hydrol. Process. 25, 448–464. https://doi.org/10.1002/hyp.7797.

van Dijk, A.I.J.M., Gash, J.H., van Gorsel, E., Blanken, P.D., Cescatti, A., Emmel, C., Gielen, B., Harman, I.N., Kiely, G., Merbold, L., Montagnani, L., Moors, E., Sottocornola, M., Varlagin, A., Williams, C.A., Wohlfahrt, G., 2015. Rainfall interception and the coupled surface water and energy balance. Agric. For. Meteorol. 214–215, 402–415. https://doi.org/10.1016/j.agrformet.2015.09.006.

Yokoo, Y., Sivapalan, M., 2011. Towards reconstruction of the flow duration curve: development of a conceptual framework with a physical basis. Hydrol. Earth Syst. Sci. 15, 2805–2819. https://doi.org/10.5194/hess-15-2805-2011.

Yue, K., De Frenne, P., Fornara, D.A., Van Meerbeek, K., Li, W., Peng, X., Ni, X., Peng, Y., Wu, F., Yang, Y., Peñuelas, J., 2021. Global patterns and drivers of rainfall partitioning by trees and shrubs. Glob. Chang. Biol. 27, 3350–3357. https://doi.org/10.1111/gcb.15644.

Zore, A., Bezak, N., Šraj, M., 2022. The influence of rainfall interception on the erosive power of raindrops under the birch tree. J. Hydrol. 613, 128478 https://doi.org/10.1016/j.jhydrol.2022.128478.